American Review of Mathematics and Statistics
December 2014, Vol. 2, No. 2, pp. 43-53
ISSN: 2374-2348 (Print), 2374-2356 (Online)

Published by American Research Institute for Policy Development
DOI: 10.15640/arms.v2n2a3
URL: http://dx.doi.org/10.15640/arms.v2n2a3

Investigation of Godunov Flux Against Lax Friedrichs' Flux for the RKDG Methods on the Scalar Nonlinear Conservation Laws Using Smoothness Indicator

Adamou M. Fode[1]

Abstract

The importance of smoothness indicator is well known in the numerical computation of hyperbolic conservation laws. The main aim is to compare and contrast Godunov flux with that of Lax-Friedrich's using smoothness indicator. We will only explore the case of smooth solutions. An example is offered to show how both fluxes behave under the TVD-RKDG scheme.

Keywords: Smoothness Indicator, Necessity of Smoothness Indicator, Numerical Smoothing, Discontinuous Galerkin Method, Conservation Laws

1. Introduction

Numerical smoothness is by now known to play a very important role in the computation of numerical solution of hyperbolic conservation law. In this paper,as stated, we use smoothness indicator -see [6]- to investigate the difference between Godunov and Lax Friedrichs' flux on smooth solutions. Consider the one-dimensional non-linear conservation laws:

$$u_t + f(u)_x = 0 \qquad (1)$$

in a bounded interval $\Omega = [a; b]$, with the initial condition $u(0; x) = uI(x)$;and the upwind boundary condition, $u(t; a) = u_a(t)$;where in this example we assume $uI(x), f(u)$, and the boundary condition to be smooth enough and consistent to guarantee that the entropy solution $u(t; x)$ is smooth near $x = a$for all $t > 0$. For simplicity we assume the case of west wind ($f'(u) > 0$).

[1]Department of Mathematics and Computer Science, Humboldt State University, Arcata, Ca 95521. Email: adamou.fode@humboldt.edu, Phone: 707 826 4203

Consider the following partition of Ω with $a = x_{-\frac{1}{2}} < x_{\frac{1}{2}} < \ldots < x_{m-\frac{1}{2}} = b$. Let $h = x_{j+\frac{1}{2}} - x_{j-\frac{1}{2}}$ be the same for all cells $\Omega_j = [x_{j-\frac{1}{2}}, x_{j+\frac{1}{2}}]$. To solve the problem with the discontinuous Galerkin method, we take the standard discontinuous piecewise polynomial space V_h. Where the degree of a local polynomial is up to p, and $V_h = \left\{v \in L^2(\Omega) : v|\Omega_j \in \prod_p\right\}$, where $\prod_p$ is the set of all the polynomials of degree less than or equal to p.

A semi-discrete solution u_h in each cell Ω_j using Godunov's flux, satisfies the following equation:

$$(u_{h,t}, v)_{\Omega_j} = (f(u), v_x)_{\Omega_j} + f(u_h(x^-_{j-\frac{1}{2}}))v(x^+_{j-\frac{1}{2}}) - f(u_h(x^-_{j+\frac{1}{2}}))v(x^-_{j+\frac{1}{2}})$$

and at the upwind boundary $x_{-\frac{1}{2}} = a$, we set $u_h(t, x_{-1/2}) = u(t, a) = u_a(t)$. While using Lax-Friedrichs' flux, in each cell Ω_j, a semi-discrete solution u_h satisfies:

$$\begin{aligned}(u_{h,t}, v)_{\Omega_j} &= (f(u), v_x)_{\Omega_j} \\ &+\tfrac{1}{2} \quad \left\{f(u_h(x^-_{j-\frac{1}{2}})) + f(u_h(x^+_{j-\frac{1}{2}})) - C[u_h(x^+_{j-\frac{1}{2}}) - u_h(x^-_{j-\frac{1}{2}})]\right\} v(x^+_{j-\frac{1}{2}}) \\ &\tfrac{1}{2} \quad \left\{f(u_h(x^-_{j+\frac{1}{2}})) + f(u_h(x^+_{j+\frac{1}{2}})) - C[u_h(x^+_{j+\frac{1}{2}}) - u_h(x^-_{j+\frac{1}{2}})]\right\} v(x^-_{j+\frac{1}{2}})\end{aligned}$$

where $C = \max_{\inf U^\circ(x) \le s \le \sup U^\circ(x)} |f'(s)|$; see [2] for more information.

At the time $t = 0$, $u_h(0, x)$ is taken to be the L_2 projection of $u_I(x)$. For the temporal discretization, we take a standard RKDG scheme of order k, see [1] in time. In this example we take $k = 3$ in the time step $[t_n, t_{n+1}]$, we compute the fully discrete solution $u^c_{n+1} \in V_h$ from u^c_n, where c stands for computed, by the following scheme. First let us use a simpler notations before given the scheme. Let

$$\begin{aligned}F^{LF}_j(u, v) &= (f(u), v_x)_{\Omega_j} \\ &+\tfrac{1}{2} \quad \left\{f(u_h(x^-_{j-\frac{1}{2}})) + f(u_h(x^+_{j-\frac{1}{2}})) - C[u_h(x^+_{j-\frac{1}{2}}) - u_h(x^-_{j-\frac{1}{2}})]\right\} v(x^+_{j-\frac{1}{2}}) \\ &-\tfrac{1}{2} \quad \left\{f(u_h(x^-_{j+\frac{1}{2}})) + f(u_h(x^+_{j+\frac{1}{2}})) - C[u_h(x^+_{j+\frac{1}{2}}) - u_h(x^-_{j+\frac{1}{2}})]\right\} v(x^-_{j+\frac{1}{2}})\end{aligned}$$

for Lax Friedrichs' flux, and

$$F^G_j(u, v) = (f(u), v_x)_{\Omega_j} + f(u_h(x^-_{j-\frac{1}{2}}))v(x^+_{j-\frac{1}{2}}) - f(u_h(x^-_{j+\frac{1}{2}}))v(x^-_{j+\frac{1}{2}})$$

for Godunov's flux. the scheme is that for $\tau_n = t_{n+1} - t_n$ and for any v in V_h, $(u^{c,1}_n, v)_{\Omega_j} = (u^c_n, v)_{\Omega_j} + \tau_n F^X_j(u^c_n, v)$,

$$(u_n^{c,2}, v)_{\Omega_j} = \frac{3}{4}(u_n^c, v)_{\Omega_j} + \frac{1}{4}(u_n^{c,1}, v)_{\Omega_j} + \frac{\tau_n}{4} F_j^X (u_n^{c,1}, v),$$
$$(u_{n+1}^c, v)_{\Omega_j} = \frac{1}{3}(u_n^c, v)_{\Omega_j} + \frac{2}{3}(u_n^{c,2}, v)_{\Omega_j} + \frac{2\tau_n}{3} F_j^X (u_n^{c,2}, v),$$

where F_j^X stands for $X = G$ or $X = LF$. At $t = 0$, we make $u_0^c = u_h(0, x)$. The upwind boundary values of $u_n^{c,1}$, $u_n^{c,2}$, u_{n+1}^c are taken according to $u_a(t)$.

2. The Smoothness Indicator

The spatial smoothness indicator contains the spatial derivatives of the computed solution u_n^c within each cell, namely

$$M_{n,j}^l = \frac{\partial^l}{\partial x^l} u_n^c(x_{j-1/2}^+).$$

The values of these $M_{n,j}^l$deliver the information about the smoothness of $u_n^c(x)$in the interior of each cell. The jumps of the derivatives across the cell boundaries is given by:

$$J_{n,j}^{l} = M_{n,j}^{l} - L_{n,j}^{l}$$

where

$$L_{n,j}^{l} = \frac{\partial^{l}}{\partial x^{l}} u_{n}^{c}(x_{j\ 1/2}^{-})$$

and for $\alpha = 1/p$,

$$D_{n,j}^{l} = \frac{J_{n,j}^{l}}{h^{p+2-l(1+\alpha)}},$$

for $j - 0, 1, \cdots, m-1$. Formally, the spatial smoothness indicator S_n^p is

$$S_n^p - \left(M_{n,j}^{l}, D_{n,j}^{l} | l - 0, 1, \cdots, p, j - 0, 1, \cdots, m-1\right).$$

The temporal smoothness indicator consist of the temporal derivatives of $u^h(t,x)$ at $t = t_n$. Namely,

$$T_n^k = \left(u_n^c, u_t^h(t_n), u_{tt}^h(t_n), \cdots, \frac{\partial^{k+1} u^h}{\partial l^{k+1}}(t_n)\right)$$

For more information on the derivation of these smoothness indicator, see [3].

As for the numerical evidence, we solve the Burgers' equation $f(u) = u^2/2$. Since we are comparing different fluxes, we will use the same initial condition $u_I(x) = 1 - (x/11)^3 sin(x)$, along with the boundary condition, $u_a(t) = 1$ for x

Table 1: The Contents of the Numerical Smoothness Indicator figures

$M_{n,j}^0$	$M_{n,j}^1$	$M_{n,j}^2$	$M_{n,j}^3$
$u_t^h = T_n^1$	$u_{tt}^h = T_n^2$	$u_{ttt}^h = T_n^3$	$u_{tttt}^h = T_n^4$
$J_{n,j}^0$	$J_{n,j}^1$	$J_{n,j}^2$	$J_{n,j}^3$
$log_h\|J_{n,j}^0\|$	$log_h\|J_{n,j}^1\|$	$log_h\|J_{n,j}^2\|$	$log_h\|J_{n,j}^3\|$

in $\Omega = [0,10]$.We also use a uniform cell size h = 0:05 with p = 3 as the order of the Legendre polynomials and the third order Runge-Kutta scheme. Note, we have reproduced the result from [6] for the purpose of this comparaison.

We will have sixteen pictures in each of the figure from 1 to 9 as shown in the table. Notice for simplicity, we drop the index j because each curve contains the values of $M_{n,j}^{l}$for $j = 0; \ldots; 199$.The solution has been computed for $t \in [0,2]$. The smoothness indicator will be shown at $t = 0.05, t = 1.05$ and $t = 2.0$ for either of the fluxes. The figures will be denoted (G) for Godonov flux cases and (FL) for Lax-Friedrich's.

Remark: We noticed that during the experiment, while Godunov's flux was conducted using $\tau = 0.005$for all the figures, the same time step size makes the scheme with Lax Friedrichs' flux very unstable. We have plotted in Figures (7)-(9) the cases where Lax-Friedrich's scheme were unstable for even a brief moment in the computation. We could clearly see that as the solution evolves, both the spatial and temporal smoothness indicator increased dramatically. The jumps are clearly getting higher and higher, and in Figure (7) we can see that the solution is just a few step away from being ruined.

To obtain the excellent result shown in Figures (b), recall those represent the solution to Lax-Friedrich's flux, we have taken the time step size to be 50% smaller than that of Godunov's time step size. Actually, using Lax-Friedrich's flux seems to fair a little better when we consider the smoothness indicator on the third row (the jumps). However the cost of even such a small accuracy

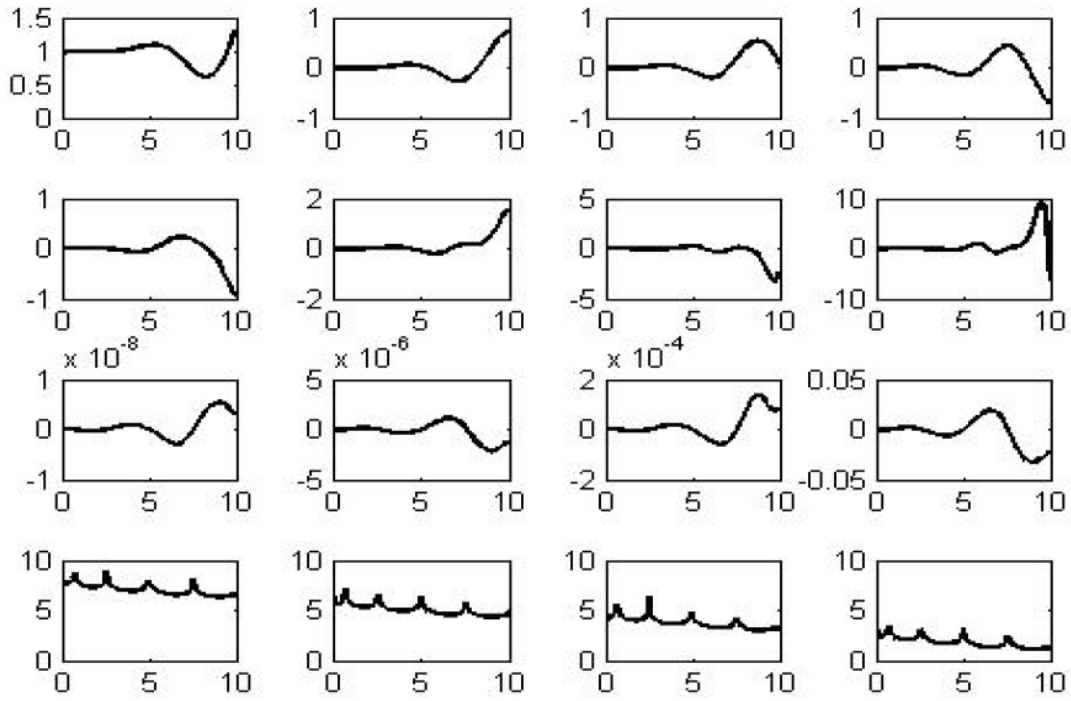

Figure 1: (G) Smoothness indicators, $\tau = 0.005$; $t = 0.05$

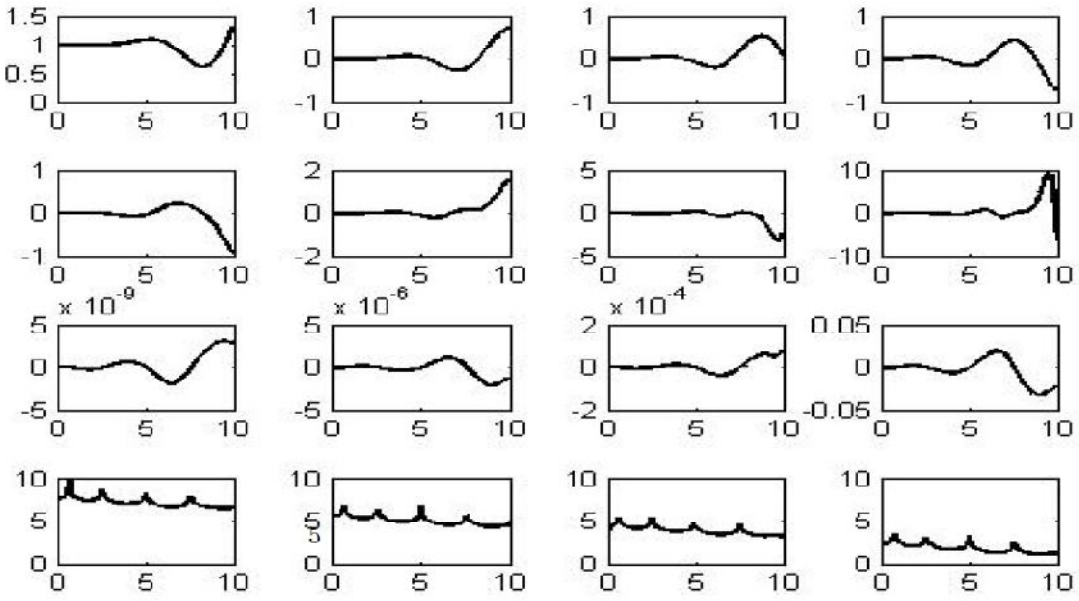

Figure 2: (LF)The Components of the Smoothness Indicator, $\tau = 0.0025$; t =0.05

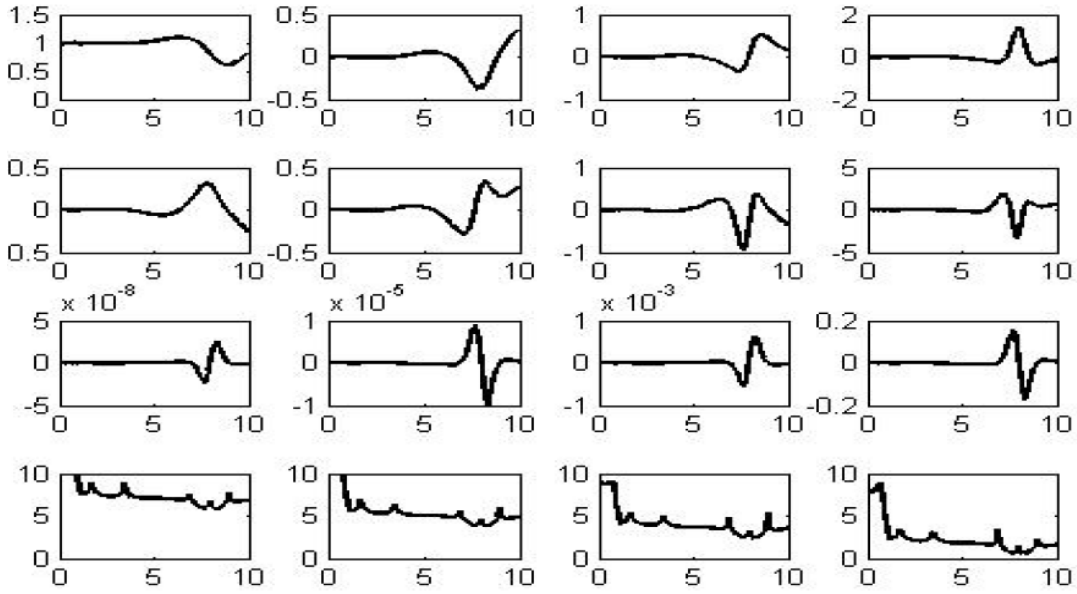

Figure 3: (G) The Components of the Smoothness Indicator,$\tau = 0.005$; t = 1.05

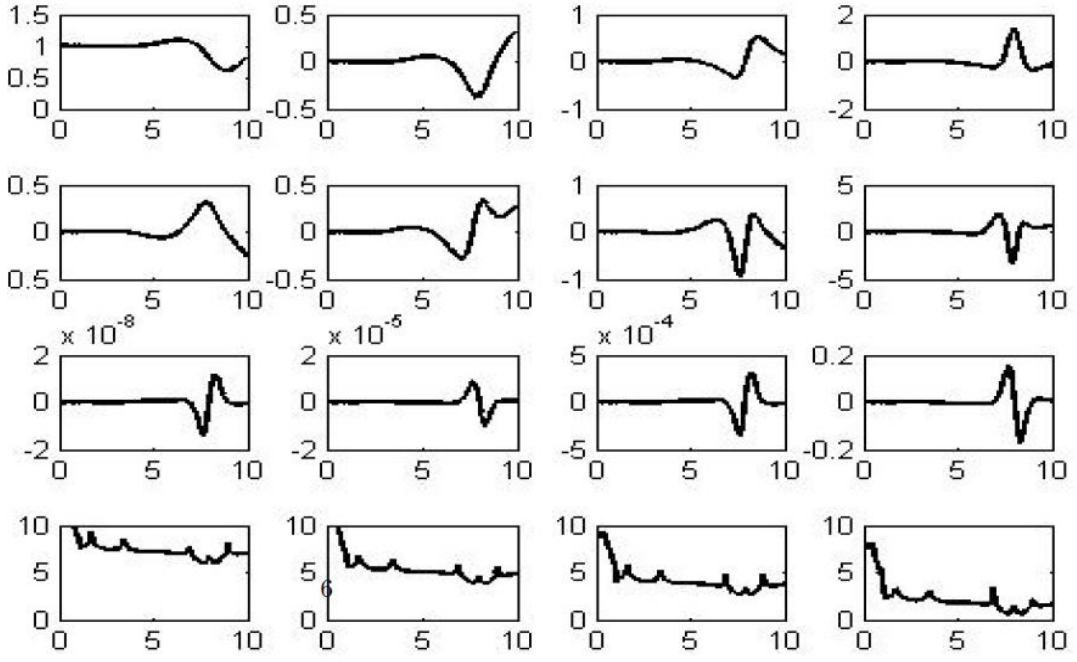

Figure 4: (LF)The components of the smoothness indicator, $\tau = 0.0025$; t =1.05

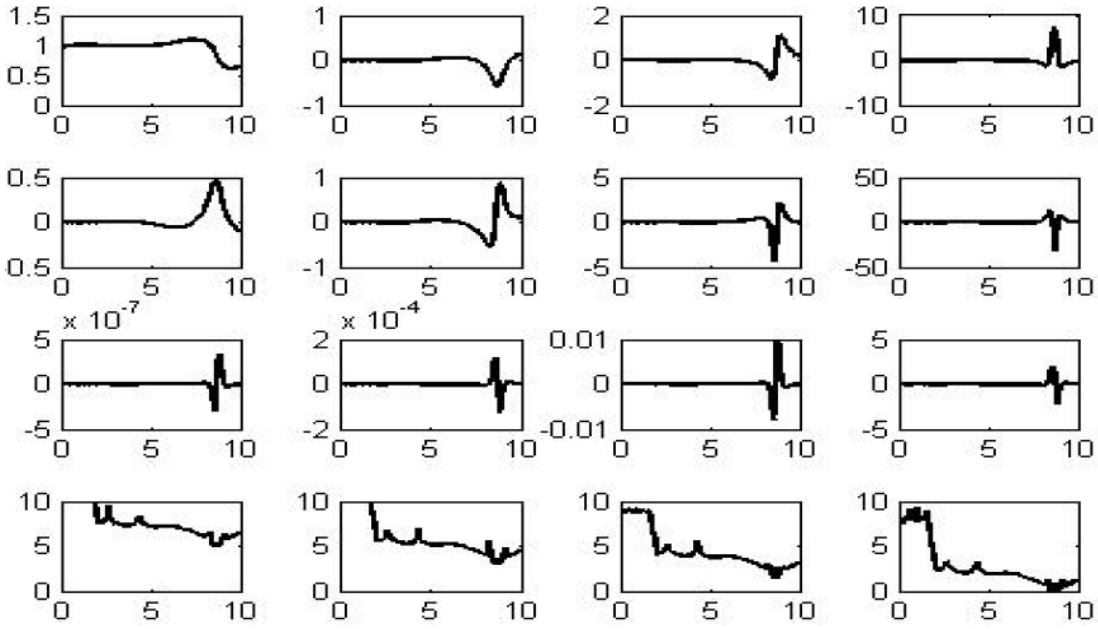

Figure 5: (G) The Components of the Smoothness Indicator, $\tau = 0.005$; t = 2

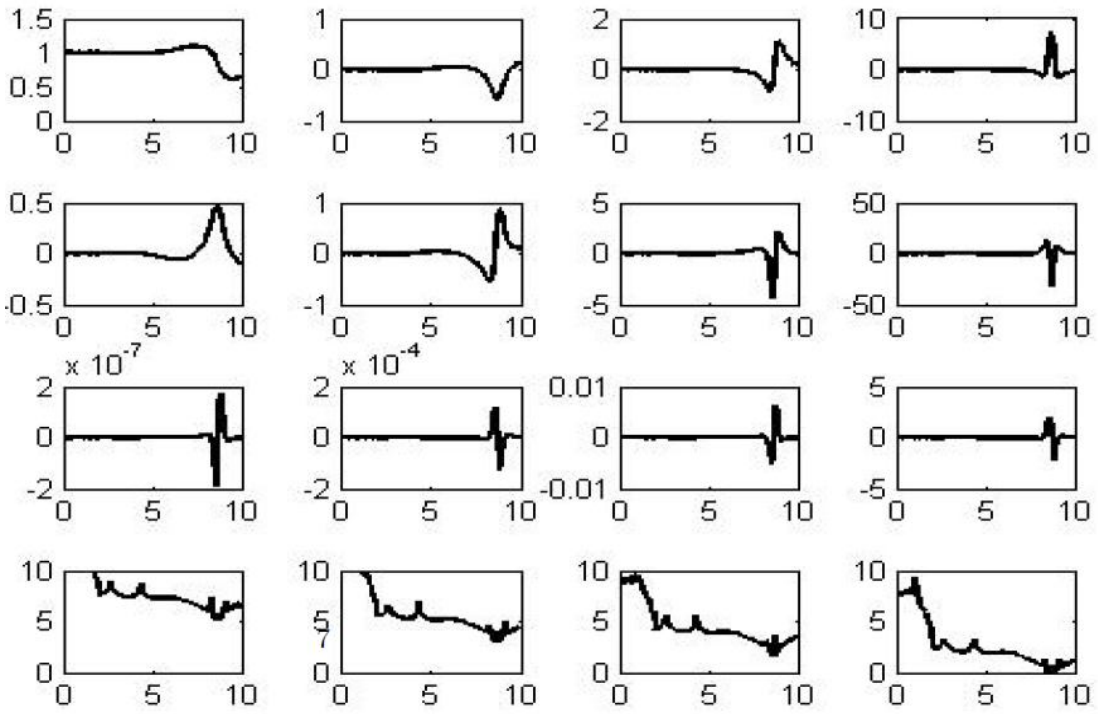

Figure 6: (LF)The Components of the Smoothness Indicator, $\tau = 0.0025$; t = 2

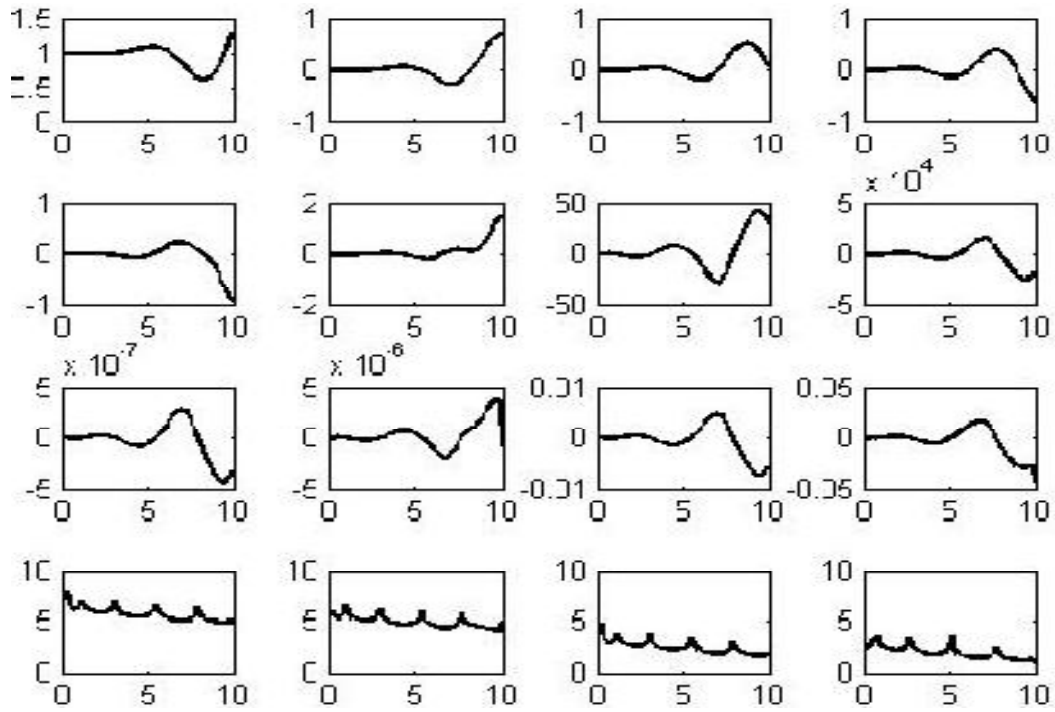

Figure 7: Lax-Friedrich, Unstable, $\tau = 0.005$; t = 0.05

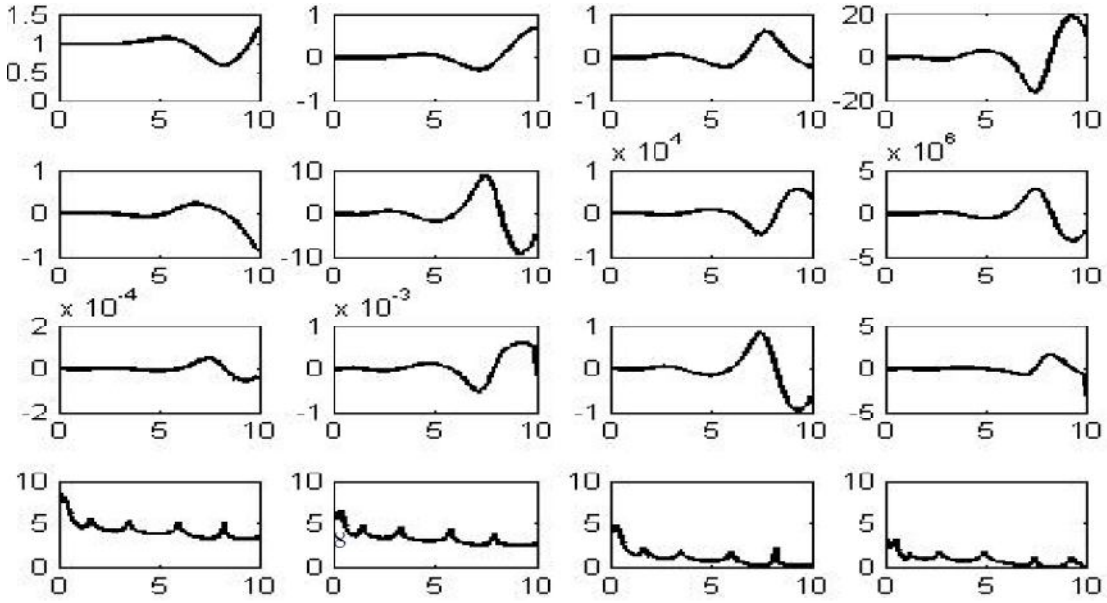

Figure 8: Lax-Friedrich, Unstable, $\tau = 0.005$; t = 0.1

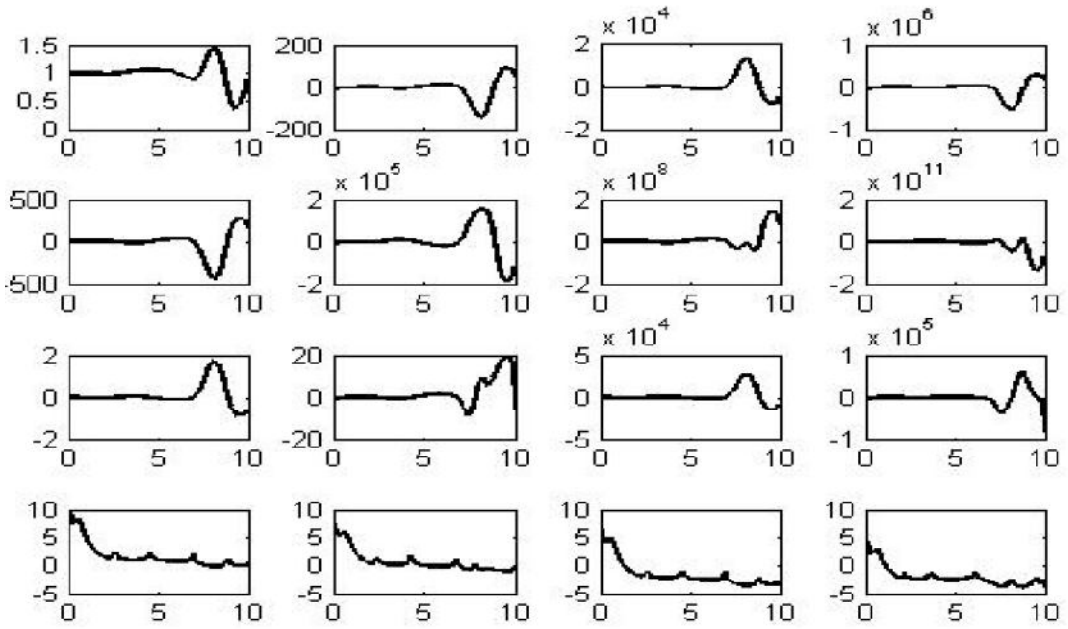

Figure 9: Lax-Friedrich, Unstable, $\tau = 0.005$; t = 0.2

is increase by taken smaller time steps. In the numerical evidence given, for Lax-Friedrichs' flux, we have taken C to be 1.45.

As shown in the numerical evidence, and as expected from the literature in partial differential equations, we have shown that both Godunov and Lax-Friedrichs fluxes behave remarkably well in their approximation of smooth solution to hyperbolic problem . It is easy to see the boundedness of the smoothness indicator in Figures (1, 2, 3 and 4) when and where the solution is smooth. However, well before the development of a shock, the third and fourth order derivatives have grown significantly in a very narrow subdomain. Soon the benefit of the approximation of high order polynomials and high order Runge-Kutta scheme will be lost, as Figures 7, 8 and 9 shows that a point of future shock is being expected soon. This numerical experiment can be extended to 2-D scalar conservation laws. The generalization of this experiment to 2-D should not have major difficulties. Moreover, this experiment could be extended to the case of a fully developped shock and contact discontinuity of various orders.

References

C.-W. Shu, Discontinuous Galerkin methods: general approach and stabil-ity,Numerical Solutions of Partial Di_erential Euations, S. Bertoluzza, S. Falletta, G. Russo and C.-W.Shu, Advanced Courses in Mathematics CRM Barcelona, Birkhauser, Basel, 2009, pp. 149-201.

T.J. Barth and H.Deconinck, (eds)High-Order Methods for Compuational Physics. Berlin; New-York:Springer, 1999.

T. Sun, A. Fode, A Discontinuous Galerkin-Front Tracking Scheme and its Optimal2 Error Estimation, submitted to arXiv for review (arXiv:1312.2519 [math.NA] 9 Dec 2013)

T. Sun, Necessity of numerical smoothness, accepted for publication in the International Journal for Information and Systems Sciences, arXiv:1207.3026v1 [math.NA], July 2012.

T. Sun, Numerical smoothness and error analysis for WENO on nonlinear conservation laws, to appear in Numerical Methods for Partial Di_erential Equations, 2013.

T. Sun and D. Rumsey, Numerical smoothness and error analysis for RKDG on the scalar nonlinear conservation laws, Journal of Computational and Ap-plied Mathematics, 241 (2013), 68-83.

T. Sun, Numerical smoothing of Runge-Kutta schemes, Journal of Compu-tational and Applied Mathematics, 233 (2009), 1056-1062.

T.J. Barth and H. Deconnick (Eds.), High-order Methds for computatioinal Physics, Lecture notes by B. Cockburn : Discontinuous Galerkin Methods for Convection-Dominated Problems, page 69 (March 1999)